Analysis of AZ31B – Ti6Al4V bimetallic extrusion by numerical simulation and Taguchi method

D Fernández[1], **A Rodríguez**[1] **and A M Camacho**[1]

[1] Department of Manufacturing Engineering, Universidad Nacional de Educación a Distancia (UNED), 28040 Madrid, Spain

*Corresponding author: dfernande146@alumno.uned.es

Abstract: This paper investigates the extrusion force and damage induced during an extrusion process to manufacture bimetallic cylinders combining a titanium alloy sleeve (Ti6Al4V) and a magnesium alloy core (AZ31B). A study has been carried out to determine the damage factor distribution through the extrusion process and how this factor together with the extrusion force are influenced by the manufacturing parameters (extrusion ratio, friction and die semi-angle) by means of finite element (FE) simulations. Also, a Taguchi Design of Experiments (DoE) and an Analysis of Variance (ANOVA) have been performed in order to study the influence of each parameter to minimize the extrusion force needed to perform the process and the damage in the extrudate. The results show that damage distribution in the sleeve does not follow any pattern, appearing in different region in a random way. However, in the core the damage always occurs in the region outside the contour of the sleeve, where it reaches the maximum value and afterwards remains stationary during the rest of the process. In the core, damage increases as friction factor does and it is independent of the cross-section reduction for low die semi-angles (15º) and reaches the maximum values for 60º die semi-angle. In both cases, damage and extrusion force, the more relevant factor to obtain minimum values is the die semi-angle.

Keywords: Extrusion, Bimetallic, Finite element method, Damage, Forces.

1. Introduction

Advanced joining and assembly processes of parts with different materials have gained relevance during lasts years, attracting great interest in sectors such as aerospace and transport due to the possibility of weight reduction which involves saving fuel, reduction of the environmental impact, and, in the case of aerospace industry, to increase the payload in aircraft and satellites. Another interesting aspect of using multi-materials in manufacturing is the possibility to customize the mechanical and thermal properties of the final part to the specific in-service requirements. For all these reasons, multi-material forming and assembly processes were identified as critical research and development area of the EU Horizon 2020 work program 2018–2020 [1].

Co-extrusion process is typically used to produce multi-material cylinders, which will be used as billets to manufacture complex shape components. This is a very complex thermo-mechanical process because of the high pressures and temperatures generated in the interface of both materials due to the plastic deformation and diffusion processes. There are several studies that involve the combination of magnesium alloys with other lightweight alloys, such as aluminium ones. An example given is Negendanka *et al.* [2] who investigated the influence of the die angle on the diffusion layer formation during coextrusion of Mg-core and Al-sleeve. Another relevant study was developed by Thirumurugan

et al. [3] and dealt with the manufacturing of an ZM21 magnesium alloy/CP aluminium using direct hot co-extrusion with three different extrusion ratios, while temperature and ram speed remained constant. Gall *et al.* [4] applied FEM simulations to co-extrusion process of bimetallic Al-Mg billets to produce hollow profiles. Unfortunately, there are only a few studies which combine such different metallic alloys in terms of density, yield strength or elastic modules, like Titanium and Magnesium alloys, as the one performed by Behrens *et al.* [5] where an analysis of semi-finished products made of aluminium and steel and manufactured by means of lateral angular co-extrusion (LACE) process was done. Or Fernández *et al.* [6] that determined the most relevant parameters to reduce the extrusion force during a co-extrusion process of bimetallic AZ31B-Ti6Al4V billets. In the other hand, none of these studies are focused in the damage induced in the parts during the co-extrusion process. Induced damage can affect the quality of the final part, its mechanical properties and its in-service performance. This damage estimation is very interesting to define favourable process conditions in order to avoid the combination of parameters that can lead to the onset of fracture. Particularly critical in extrusion is the defect called "chevron cracking" also known as "central burst" because it is an internal defect and it cannot be detected by visual inspection techniques. Again, there are several studies about central bursting in extrusion like the ones carried out by Parghazeh *et al.* [7] predicting the defects in rod extrusion process by means of upper bound analysis method or Reddy *et al.* [8] about obtaining an optimal die profile to reduce the central bursting in axisymmetric extrusion. All these studies are focused in single material extrusion; it is possible to find articles about quality of the final part of a multi-material component after coextrusion process like Berski *et al.* [9], but again damage distribution is barely mentioned. Special mentions are the studies about prevention of core and sleeve fracture of bimetal rods performed by Avitzur *et al.* [10,11] and safety maps in bimetallic extrusions by Alcaraz *et al.* [12] and Amigo *et al.* [13].

This study focuses on forces and damage distribution in coextrusion process of bimetallic AZ31B-Ti6Al4V billet considering the manufacturing parameters die semi-angle, extrusion relation and friction between container and sleeve. An ANOVA was performed in order to establish which of these manufacturing parameters are more significant to reduce the damage but also to minimize the extrusion force required. Cockcroft-Latham criterion [14] has been applied during simulations.

2. Materials and Methods

2.1. Materials, Geometrical Dimensions and Process Parameters

The materials used in the simulations for the bimetallic cylinders are the following:

- Magnesium alloy UNS M11311 (AZ31B) for the core.
- Titanium alloy UNS R56400 (Ti6Al4V) for the sleeve.

The election of these materials bases mainly on the difference in density of both materials, which is almost 4 times higher in titanium alloy.

Main physical and mechanical properties of both materials are listed in table 1 [15-16].

Table 1. Physical and nmechanical properties titanium alloy Ti6Al4V and magnesium alloy AZ31B.

Property	Ti6Al4V	AZ31B
Density (g/cm^3)	4.46	1.74
Tensile strength (MPa)	895	260
Yield strength (MPa)	828	200
Elastic modulus (GPa)	105 – 120	44.80
Poisson's ratio	0.31	0.35

The initial bimetallic cylinder geometrical dimensions are presented in figure 1.

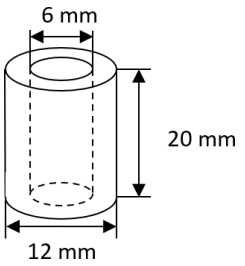

Figure 1. Bimetallic cylinder geometrical dimensions.

2.2. Finite Element Modelling

Finite element simulations have been performed using the commercial finite element software DEFORM3D©. In order to reduce computation time, only a quarter of the process was modelled because of axial symmetry of the problem. Sleeve and core were modelled as plastic objects while ram and container were done as rigid ones. The friction model used in all simulations was the shear friction model, which considers a constant friction factor *m* and it only depends on the shear flow stress *k* according with equation (1).

$$r = m \cdot k \tag{1}$$

Shear friction model is probated more realistic that Coulomb's one in modelling forming operations [17].

The method chose for estimating the damage factor is the normalized Cockcroft and Latham criterion, which is mainly used for predicting damage in metal forming operations [18] because of its simplicity and the accessibility of material data needed for the calculation. This criterion is based on the hypothesis that the accumulation of damages occurs only when at least one of the principal stress components is tensile and it stablishes that fracture occurs in a ductile material when the integral in equation (2) reaches a constant value, C, for a given temperature and strain rate. DEFORM3D© calculates the damage values during the process by solving the integral in each step

$$\int_0^{\varepsilon_f} \left\langle \frac{\sigma_{max}}{\sigma_H} \right\rangle d\varepsilon = \tag{2}$$

where ε is the equivalent plastic strain, ε_f is the equivalent strain to fracture, σ_{max} is the maximum principal stress, σ_H is the stress according to the Huber – Misses hypothesis and *C* is a constant depending on the material and experimental determined. Materials AZ31B and Ti6Al4V were assumed to be isotropic during all the process. Plastic parts were meshed using 7000 tetrahedral elements and the model was validated by Fernández *et al.* [6] by comparing the simulations results for the extrusion force with the results using Johnson semi-empirical model [19,20].

2.3. Methodology

For this paper only parameters related to the tooling have been taken into account to perform the different simulations. The reason is the direct impact on the design of the container/die and, therefore on the cost of the initial investment. The values considered for temperature, ram speed as well as dimensions of the billet (see figure 1) have been taken from Fernández *et al.* [6] and are the following ones:

- Temperature = 200 ºC
- Ram speed = 2 mm/s

Both temperature and ram speed as fixed as an input parameters and heat exchange among parts is allowed during simulations.

The extrusion relation, or reduction relation, has been calculated by equation (3) [21]:

$$R_E = A_o/A_f \quad (3)$$

where A_o is the initial area and A_f is the final one.

A DoE has been performed using Taguchi method [22] to obtain an orthogonal array for three factors with two levels L4 (23).

Finally, an ANOVA is used to calculate the signal to noise (S/N) by equation (4) taking into account the condition that the lower the better:

$$S/N = -10 \log [(1/n) \cdot (\Sigma y^2)] \quad (4)$$

where y is the observed data and n the number of observations

Table 2 shows the Taguchi's orthogonal array L4 (2^3).

Table 2. Taguchi's orthogonal array for damage factor and extrusion force.

Simulation	Die semi-angle (°)	Friction	R_E	Maximun damage value	Extrusion force (kN)
1	15	0.1	1.44	2.07	82.94
2	15	0.3	1.78	2.51	122.85
3	45	0.1	1.78	0.98	130.35
4	45	0.3	1.44	0.86	164.84

3. Results and discussion

According to simulations, two different damage distributions can be found during the extrusion process. One regarding to titanium alloy sleeve and one for magnesium alloy core.

Damage distribution in the sleeve does not follow any pattern during the forming process, therefore the study will be focused on what happens in the core. Figure 2 shows damage distribution in the core.

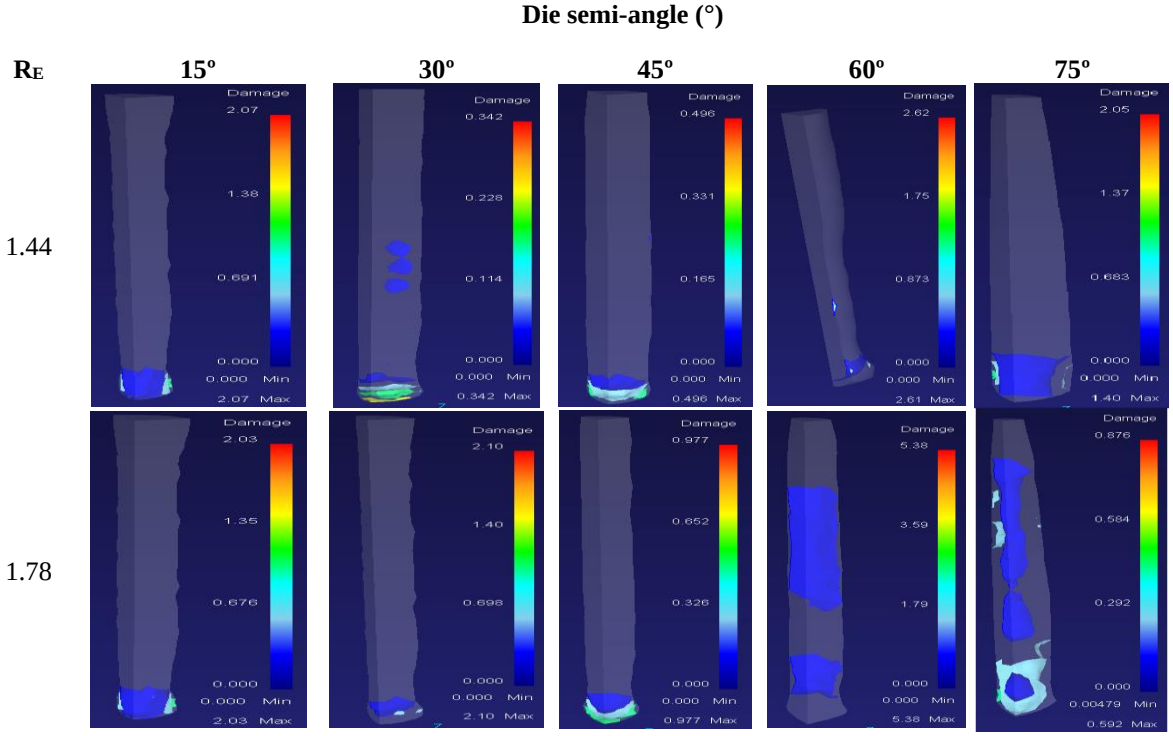

Figure 2. Damage distribution in the core for different R_E at several die semi-angles.

Contrary to what happened in the sleeve, core damage has a defined region of occurrence and its distribution in general (exceptions will be explained later) once it reaches the highest value remains stationary during the rest of the process.

Figure 3 shows the damage evolution during the extrusion process for different die semi-angles and extrusion relations.

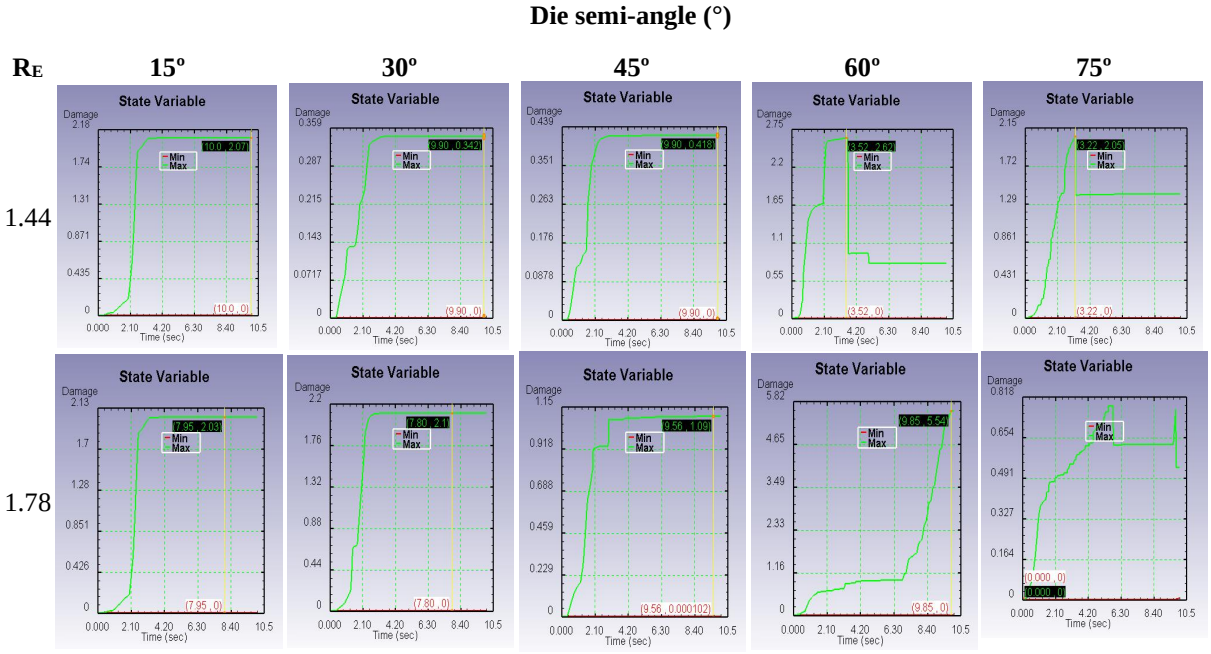

Figure 3. Core damage distribution at different die semi-angles and extrusion relations.

For low extrusion relations and die semi-angles values up to 45º, damage in the core growths very quick during the first steps until it reaches a peak where remains constant until the end of the process. On the other hand, in this sense, 60º die semi-angle is identified as critical because from this point onwards the damage reaches a peak and an immediate descent until it reaches a permanent regime. The reason behind this can be explained by the dead zone formation for high values of the die semi-angle. Particularly interesting is the case for 60º and R_E = 1.78 in figure 2 where the damage increases exponentially, which can mean the formation of the chevron crack. Damage is associated to stress states, mainly because the hydrostatic stress as it's explained in the hydrostatic stress criterion (HSC) that says "whenever hydrostatic stress at a point on the centre line in the deformation zone becomes zero and it is compressive elsewhere, there is a fracture initiation leading to central burst" [8]. Figure 4 shows the damage variation depending of the extrusion relation (R_E) for each die semi-angle.

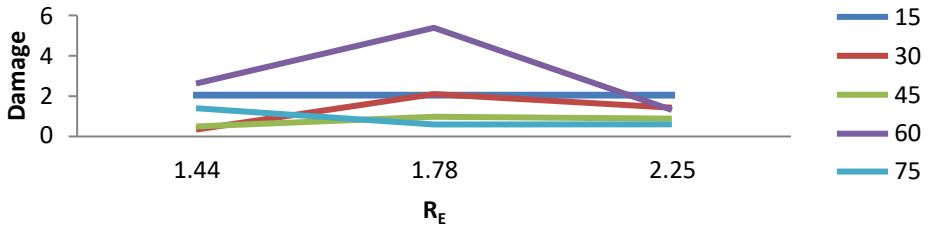

Figure 4. Damage versus extrusion relation at different die semi-angles (º).

This graph reinforces the importance of 60º die semi-angle as critical one. For very low semi-angles, damage factor remains constant independent of extrusion relation, as is the case for 15 º. There is a pattern of increase of damage factor with the increase of extrusion relation for semi-angles 30º and 45º. However, from 60º onwards there is no clear relation between damage factor and extrusion relation, as it was mentioned before the most likely cause is the formation of the dead zone for these semi-angle values. Finally, there is not too much variation in damage factor at medium/high die semi-angles for high extrusion relation values. A safety area has been established in figure 5 to ensure that damage values remain as low as possible during the extrusion process.

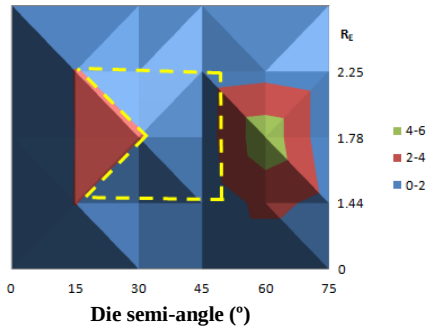

Figure 5. Damage map.

Regarding the influence of the shear friction on the core damage factor, figure 6 shows that, although damage increases as the friction factor does, there are three different regions with their own behaviour. In region I damage increases linearly with a slope of 2, while region II damage remains practically constant and in region III damage increases exponentially reaching between three and four times the values obtained in region I.

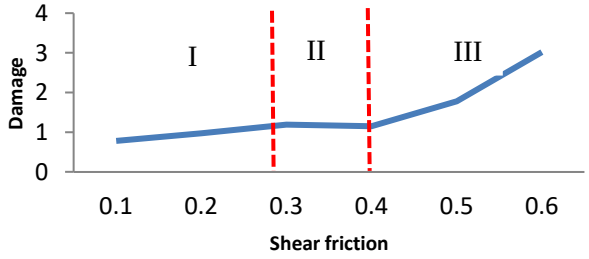

Figure 6. Damage distribution at different shear friction values.

Finally, after applying ANOVA to the orthogonal array showed in table 2, it can be concluded that the most relevant factor to obtain a low damage factor in the core and requires low values for the extrusion force is the die semi-angle, as table 3 and 4 shows.

Table 3. Taguchi's results for the average values of the damage factor and extrusion force.

	Damage Factor			Extrusion Force		
Level	Die semi-angle	Friction	R_E	Die semi-angle	Friction	R_E
1	2.29	1.52	1.46	-7.24	-4.18	-4.00
2	0.92	1.68	1.74	-0.73	-5.46	-5.60
Delta	1.37	0.16	0.28	7.96	1.28	1.60
Classification	1	3	2	1	3	2

Table 4. Taguchi's results for the noise signal values of the damage factor.

	Damage Factor			Extrusion Force		
Level	Die semi-angle	Friction	R_E	Die semi-angle	Friction	R_E
1	-7.24	-4.18	-4.00	-40.41	-40.77	-42.31
2	-0.73	-5.46	-5.60	-43.44	-43.25	-42.05
Delta	7.96	1.28	1.60	3.03	2.48	0.26
Classification	1	3	2	1	2	3

4. Conclusions

According with the results presented in this paper, a robust FE model for AZ31B – Ti6Al4V bimetallic co-extrusion has been used to estimate the induced damage and the extrusion force during the process for different manufacturing parameters while ram speed and temperature are maintained as it is explaining in section 2.3 Methodology. Sleeve damage has been proved as random with no clear zone of appearance or a pattern for the appearance of maximum or minimum values. Core damage is focus in the region outside the contour of the sleeve and for low/medium extrusion relations and angles below of 60º when the damage reaches its maximum value it remains stationary for the rest of the process. Die semi-angle of 60º has been identified as critical because from this value the formation of the dead zone causes random distribution of the damage and in one case (60º and a extrusion reduction of 1.78) a possible chevron crack defect. For low die semi-angles as 15º, damage factor is independent of the extrusion relation. For high extrusion relations damage factor has no significant variation at die semi-angles above 15º. Regarding friction, damage factor increases as the friction coefficient does, reaching a stationary state from values between 0.3 and 0.4. For friction values higher than 0.4 the damage increases exponentially. Finally, the most relevant manufacturing parameter to reduce the damage factor in the core is the die semi-angle as well as to obtain minimum values for the extrusion force which are very useful to reduce the power requirement of the machinery to invest in.

The results of this paper can potentially be used to improve the quality of the extrudates and, along with the use of lightweight materials, can contribute to sustainable production approaches by reducing fuel consumption of the vehicles made of them and thus the environmental impact.

Acknowledgements

This work was developed within the framework of the Doctorate Program in Industrial Technologies of the UNED and was funded by the Annual Grants Call of the E.T.S.I.I. of the UNED via the project References 2021-ICF07 and 2021-ICF08 and by the Innovation Teaching Project of the GID2016-28 focused on "Reliability and Advanced Failure Prognosis applied to the teaching of Materials Technology and Processing".

References

[1] European Comission Horizon 2020 *Work Programme 2018-2020 5.ii. Nanotechnologies, Advanced Materials, Biotechnology and Advanced Manufacturing and Processing* (https://ec.europa.eu/research/participants/data/ref/h2020/wp/2018-2020/main/h2020-wp1820-leit-nmp_en.pdf) accessed 3 March 2021

[2] Negendanka M, Mueller S and Reimers W 2012 Coextrusion of Mg-Al macrocomposites *Journal of Material Process Technology* **212** (9) pp 1954–1962

[3] Thirumurugan M, Anka Rao S, Kumaran S and Srinivasa Rao T 2011 Improved ductility in ZM21 magnesium-aluminium macrocomposite produced by co-extrusion *Journal of Material Process Technology* **211** pp 1637–1642

[4] Gall S, Müller S and Reimers W 2009 Aluminum coating of magnesium hollow profiles by using the coextrusion process *Aluminum International Journal* **85** pp 63–67

[5] Behrens B A, Klose C, Chugreev A, Heimes N, Thürer S E and Uhe J 2018 A numerical study on co-extrusion to produce coaxial aluminium-steel compounds with longitudinal weld seams

Metals **8** p 717
[6] Fernández D, Rodríguez-Prieto A and Camacho A M 2020 Effect of Process Parameters and Definition of Favorable Conditions in Multi-material Extrusion of Bimetallic AZ31B-Ti6Al4V Billets *Appl. Sci.* **10** (22) p 8048
[7] Parghazeh A and Haghighat H 2016 Prediction of central bursting defects in rod extrusion process with upper bound analysis method *Transactions of Nonferrous Metals Society of China* **26** (11) pp 2892–2899.
[8] Reddy N V, Dixit P M and Lal G K 1996 Central bursting and optimal die profile for axisymmetric extrusion *J. Manuf. Sci. Eng.-Trans. ASME* **118** pp 579–584
[9] Berski S, Dyja H, Maranda H, Nowaczewski J and Banaszek G 2006 Analysis of quality of bimetallic rod after extrusion process *Journal of Materials Processing Technology* **177** pp 582–586
[10] Avitzur B, Wu R, Talbert S and Chou Y T 1982 Criterion of the prevention of core fracture during extrusion of bimetal rods ASME *J. Eng. Ind*. **104** p 292
[11] Avitzur B, Wu R, Talbert S and Chou Y T 1986 Criterion of the prevention of sleeve fracture during extrusion of bimetal rods ASME *J. Eng. Ind.* **108** p 205
[12] Alcaraz J L and Gil-Sevillano J 1996 Safety maps in bimetallic extrusions *Jornal of Materials Processing Technology* **60** pp 133–140
[13] Amigo F and Camacho A M 2017 Reduction of induced central damage in cold extrusion of dual-phase steel DP800 using double-pass dies *Metals* **7** (9) p 335
[14] Cockcroft M G and Latham D J 1968 Ductility and the workability of metals *J. Inst. Metals* **96** pp 33–39
[15] Avedesiam M and Baker H 1999 *Magnesium and magnesium alloys ASM speciality handbook* (Ohio, USA)
[16] Donachie M J 1988 *Titanium. A technical guide ASM International* (USA)
[17] Zhang D W and Ou H 2016 Relationship between parameters in a Coulomb-Tresca friction model for bulk metal forming *Tribol. Int*. **95** pp 13–18
[18] Stebunox S, Vlasov A and Biba N 2018 Prediction of the fracture in cold forging with modified Cockcroft-Latham criterion *Procedia Manuf* **15** pp 519–526
[19] Johnson W 1956-1957 The pressure for the cold extrusion of lubricated rod through square dies of moderate reduction at slow speeds *Journal of the Institute of Metals* **85** pp 403–408
[20] García-Domínguez A, Claver J, Camacho A M and Sebastián M A 2015 Comparative analysis of extrusion processes by finite elements analysis *Procedia Eng* **100** pp 74–83
[21] M P Groover 2010 *Fundamentals of modern manufacturing* (New Jersey, USA: John Wiley & Sons)
[22] Gisbert C, Bernal C and Camacho A M 2015 Improved analytical model for the calculation of forging forces during compression of bimetallic axial assemblies *Procedia Eng* **132** pp 298–305
[23] Scientific Forming Technologies 2017 *DEFORM v11.2 User's Manual Scientific Forming Technologies Corporation* (Columbus Ohio, USA)